

FORCE BALANCE IN OUTER PLANET MAGNETOSPHERES

R. L. McNutt, Jr.

Department of Physics and Center for Space Research, M.I.T.
Cambridge, Massachusetts 02139

ABSTRACT

Spacecraft measurements near Jupiter and Saturn have revealed strong planetary magnetic fields which contain significant amounts of plasma. The magnetospheres which result are corotation dominated and the plasma distribution is in a quasi-steady state. Assuming azimuthal symmetry and time independence, data obtained in situ can be used to investigate the validity of the MHD momentum equation in these rapidly rotating magnetospheres. We find that both centrifugal and pressure gradient forces must be considered. At both Jupiter and Saturn currents flowing in the magnetosphere produce substantial modifications of the planetary magnetic fields. The particle measurements and the assumption of stress balance place strict requirements on these magnetospheric current systems. In comparing our results with models of the field we find that the best model of the magnetic field of the current sheet at Jupiter produces too much inward Lorentz force relative to the outward centrifugal and pressure gradient forces. A similar model for the ring current in Saturn's magnetosphere produces a Lorentz force in much better agreement with that required by particle measurements. A simple model of stress balance along field lines does not hold at either Jupiter or Saturn outside of ~ 10 planetary radii. General considerations suggest that the configurations of fields and distributions of particles at Uranus and Neptune may be similar to those found at Jupiter and Saturn.

INTRODUCTION

Magnetic field lines which emanate from rotating, magnetized celestial objects tend to enforce their own angular velocity upon the plasma which they thread in the space outside the object. If plasma at the feet of the field lines has the same angular velocity as the celestial body, the entire magnetosphere - field and plasma - will rigidly corotate with the central object [1,2,3,4].

Plasma brought up to this angular velocity experiences an outward centrifugal force in the corotating frame of reference. This force drives an azimuthally directed current in the rest frame of the plasma such that the resulting $\vec{J} \times \vec{B}$ force balances the centrifugal force and leads to a state of equilibrium [5]. Plasma injected into a planetary magnetosphere

can produce such a current provided that there is sufficient transfer of torque from the rotating planet to its highly conducting ionosphere [5,6,7].

This "ring current" produced by the plasma inertia, in turn produces its own magnetic field which modifies that of the central object, and distends the magnetic field lines relative to those of the vacuum field. Alternatively, one can think of the plasma as "stretching" the original field lines outward until the magnetic tension balances the centrifugal force on the rotating plasma.

The rapid rotation rate and inferred magnetic field of Jupiter led Piddington in 1969 [8] to postulate that Jupiter would have an "inflated" magnetosphere. Brice and Ioannidis [9] concluded that essentially all of Jupiter's magnetosphere should be closed and corotating, i.e., that the Jovian plasma-sphere would fill the entire magnetosphere at Jupiter.

In 1973, the Pioneer 10 encounter with Jupiter revealed a magnetosphere which extended about twice as far from Jupiter as expected. Smith et al. [10] postulated that the distention resulted from a relatively cold, dense, corotating plasma undetected by Pioneer. Subsequent modeling of the Pioneer 10 magnetic field data suggested that such a corotating plasma must instead be hot (on the order of 10 keV in temperature) [11,12,13], and analysis of Pioneer data by Walker et al. [14] showed that the diamagnetic effect of such a hot plasma could explain the depressions observed in the magnetic field intensity. These occurred during "crossings" of the current sheet by the spacecraft as it moved between high and low magnetic latitudes along its trajectory.

Prior to the Pioneer 11 encounter with Saturn in 1980, arguments similar to those applied to the Jovian system suggested that a Kronian magnetosphere should be essentially a scaled down version of the Jovian one [15,16]. The Pioneer 11 measurements showed that Saturn does possess a magnetic field and substantial amounts of plasma were detected close to the planet [17]. Nevertheless the contribution of local currents to the field was assumed to be negligible [18] and the field in the magnetosphere was thought to be that of the planet alone.

More detailed measurements of the planetary magnetic fields and plasma populations at Jupiter (1979) and Saturn (1980, 1981) by the Voyager spacecraft have allowed a better assessment of the relative importance of "hot" and "cold" plasma to magnetospheric dynamics. In addition, a more quantitative evaluation of the balance of stresses as determined by

north spin and magnetic poles in the same hemisphere \hat{b} points southward and \hat{n} points outward at the equatorial plane. No azimuthal magnetic field component and azimuthal symmetry imply $\vec{J} = J\hat{\phi}$. Then $\vec{J} \times \vec{B} = -JB\hat{n}$. Define $\partial/\partial\lambda \equiv -b \cdot \nabla$ and $\partial/\partial s \equiv (b \times \phi) \cdot \nabla$. The components of Eq. (5) along and across the field are, respectively [34]:

$$\frac{\partial}{\partial\lambda} (\ln P_{\parallel}) = \frac{\rho}{P_{\parallel}} \frac{\partial}{\partial\lambda} \left(\frac{1}{2} \Omega \tilde{\omega}^2 \right) + \left(1 - \frac{P_{\perp}}{P_{\parallel}} \right) \frac{\partial}{\partial\lambda} (\ln B) \quad (6)$$

(N.B. $\frac{\partial\Omega}{\partial\lambda} = 0$) and

$$\begin{aligned} \rho\Omega^2 \frac{\partial}{\partial s} \left(\frac{1}{2} \tilde{\omega}^2 \right) &= \frac{\partial P_{\perp}}{\partial s} + (P_{\parallel} - P_{\perp}) \frac{\partial}{\partial s} (\ln B) \\ &+ \frac{1}{c} JB \left[1 - \frac{4\pi}{B^2} (P_{\parallel} - P_{\perp}) \right] \end{aligned} \quad (7)$$

All quantities are now to be treated as functions of λ and s . Eqs. (6) and (7) relate various quantities for a given magnetic field configuration which is not known a priori.

We can effect a simplification near the symmetry surface. By symmetry B_{\parallel} must be an odd function of z and B_{\perp} must be an even function. Near $z = 0$, $\lambda = z + O(z^3/\tilde{\omega}^2)$ and $s = \tilde{\omega} + O(z^2/\tilde{\omega}^2)$. Eq. (6) becomes (to first order in z):

$$\frac{\partial(\ln P_{\parallel})}{\partial(z^2)} = \frac{1}{h^2} \quad (8)$$

$$\frac{1}{h^2} = \frac{\rho}{2P_{\parallel}} \frac{\Omega^2 \tilde{\omega}}{R_c} - \frac{1}{2R_c} \frac{\partial(\ln P_{\parallel})}{\partial \tilde{\omega}} + \frac{1}{2} (P_{\perp}/P_{\parallel} - 1) \left(\frac{1}{\tilde{\omega}} \frac{\partial \tilde{\omega}}{\partial \tilde{\omega}} \left[\frac{\tilde{\omega}}{R_c} \right] + \frac{1}{R_c^2} \right) \quad (9)$$

In Eq. (9) R_c is the radius of curvature of the field lines at $z=0$. If the plasma temperatures are constants, Eq. (8) can be integrated to give a gaussian profile; h is then usually called the centrifugal scale height [34,37,38].

Similarly, we can show that to first order in z , Eq. (7) can be written as

$$\rho\Omega^2 \tilde{\omega} = \frac{\partial P_{\perp}}{\partial \tilde{\omega}} + (P_{\parallel} - P_{\perp}) \frac{\partial(\ln B)}{\partial \tilde{\omega}} + \frac{1}{c} JB \left(1 - \frac{4\pi}{B^2} [P_{\parallel} - P_{\perp}] \right) \quad (10)$$

Define the Alfvén Mach number by $M_A^2 \equiv 4\pi\rho\Omega^2\tilde{\omega}^2/B^2$ and the parallel and perpendicular β 's by $\beta_{\parallel} \equiv 8\pi P_{\parallel}/B^2$. After some manipulation we can rewrite Eq. (10) as [39]:

$$M_A^2 = \frac{1}{2} \beta_{\perp} \frac{\partial(\ln P_{\perp})}{\partial(\ln \tilde{\omega})} + \frac{1}{2} (\beta_{\parallel} - \beta_{\perp}) \frac{\partial(\ln B)}{\partial(\ln \tilde{\omega})} + \frac{4\pi \tilde{\omega} J}{c B} \left(1 - \frac{1}{2} [\beta_{\parallel} - \beta_{\perp}]\right) \quad (11)$$

Eqs. (8), (9) and (11) are the stress balance equations near the symmetry surface for a confined, rotating magnetosphere. In this form, the magnetic field must be globally specified. We can obtain the current density and field line curvature from the given field by using

$$\frac{1}{R_c} = \frac{1}{B_z} \left. \frac{\partial B_{\tilde{\omega}}}{\partial z} \right|_{z=0} \quad (12)$$

and

$$\frac{4\pi}{c} J = B \left(\frac{1}{R_c} + \frac{\partial[\ln B]}{\partial \tilde{\omega}} \right) + O(z^2) \quad (13)$$

where we have made use of

$$B(z, \tilde{\omega}) = - B_z(\tilde{\omega}) \Big|_{z=0} + O(z^2) \quad (14)$$

The literature is rich in various magnetic field models for Jupiter [34]. The ring current or current sheet model of Connerney, Acuna, and Ness (hereafter CAN) has been used to model magnetometer data obtained by both Voyager 1 and Voyager 2 during their encounters with both Jupiter and Saturn [40,41]. The CAN model assumes an azimuthal current of strength $J = I_0 \int_{\tilde{\omega}}^{\infty}$ flowing in an annulus of inner radius a , outer radius b , and half-thickness D . The dimensions of the annulus as well as I_0 are parameters which are adjusted by comparison with magnetometer data obtained in situ. The total magnetic field is found by combining the field of the current sheet and the appropriate multipole representation of the internal planetary field.

For the magnetospheric regions of interest here, we can simply assume that the planetary fields are dipolar. The exact expression for the sheet field can only be reduced to quadrature. However, it can be shown that a very good approximation is

$$B_{z, \text{sheet}}(\tilde{\omega}, z=0) = \frac{4\pi I_0}{c} \frac{2D}{\pi} [f(\tilde{\omega}, D, a) - f(\tilde{\omega}, D, b)] \quad (15)$$

where

$$f(\tilde{\omega}, D, x) \equiv \frac{1}{([\tilde{\omega} + x]^2 + D^2/4)^{1/2} K\left(\left[\frac{4\tilde{\omega}x}{(\tilde{\omega} + x)^2 + D^2/4}\right]^{1/2}\right)} \quad (16)$$

and $K(k)$ is the complete elliptic integral of the first kind [42]. This approximation yields an error in the total field of $\leq 1\%$ for $a \leq \omega \leq 0.85 b$ and an error of $\leq 9\%$ for $0.85 b \leq \omega \leq b$ at Jupiter and an error of $\leq 12\%$ for $a \leq \omega \leq b$ at Saturn (this is a much better approximation than that obtained in ref. [40]). Note that fields produced by magnetopause and magnetotail currents have been neglected; this is probably not serious for the region $\omega \leq b$. Using the CAN current sheet model and Eqs. (13)-(16) we can also obtain an analytic approximation for $R_0(\tilde{\omega})$. This supplies us with the necessary information about the magnetic field required to investigate force balance near the symmetry surface.

VOYAGER AT JUPITER

Comparisons of experimented data and the theoretical relations derived in the previous section are limited by the spacecraft trajectory, viewing directions of the PLS [43] and LECP [44] experiments, and the current state of analysis of the data. The fixed orientation of the PLS experiment with respect to the Voyager spacecraft limits the comparison at this time to the data obtained along the inbound trajectories of the two spacecraft [24]. Voyager 1 and Voyager 2 crossed the symmetry surface of the Jovian magnetosphere twice each rotation period, roughly once every five hours as a result of the 9.6° tilt between the magnetic and rotational axes. This tilt also gives rise to a symmetry surface for cold plasma, the "centrifugal equator" [45], the axis of which is tilted about two thirds that of the magnetic axis from the spin axis. Centering the model current sheet on the centrifugal rather than the magnetic equator provides a better match of the CAN model field to the Voyager magnetometer data obtained by Voyager 1 [46]. This suggests a simple symmetry for the magnetosphere.

The tilt has apparently introduced additional plasma dynamical effects, however, which are evident in the first two figures. Fig.(1) shows high resolution (M-mode) data obtained by the PLS experiment on Voyager 1 between $\sim 33 R_J$ and $20 R_J$ inbound.

Fig. 2 shows equivalent data between $\sim 22 R_J$ and $10 R_J$ inbound on a different scale. Crossings of the magnetic symmetry surface are indicated.

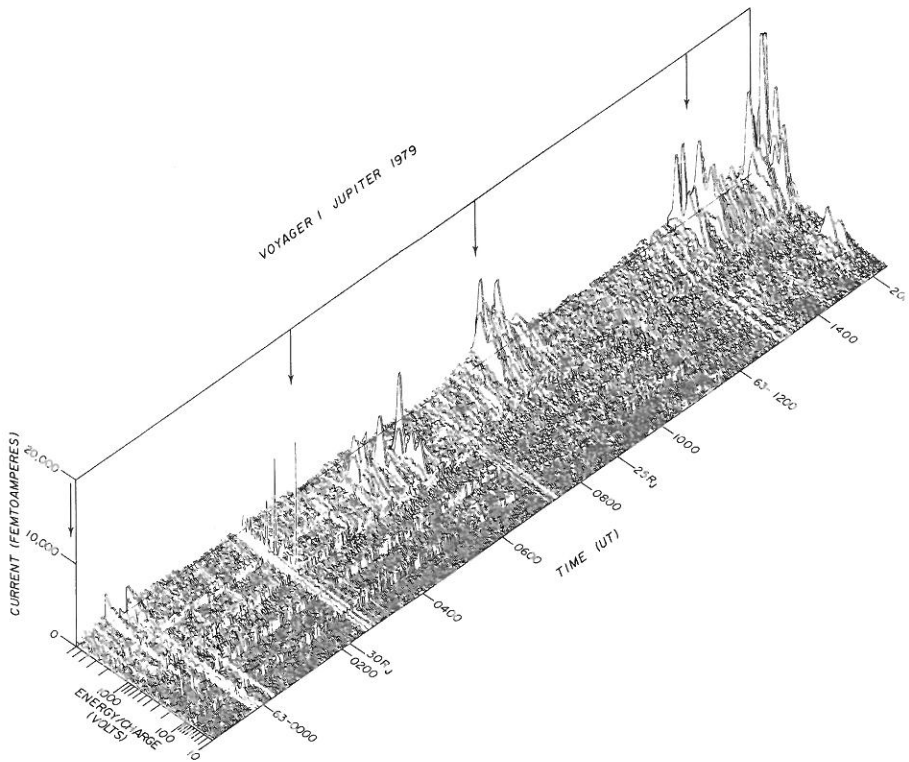


Fig. 1 Voyager 1 data acquired at Jupiter by the side sensor of the PIS experiment. The maximum current displayed is 2×10^{-11} amperes (see [43]). This corresponds to a charge flux density of $\sim 2.2 \times 10^6$ electron charges $\text{cm}^{-2} \text{s}^{-1}$. The arrows indicate crossings of the magnetic equatorial plane.

The most striking features which cannot be explained on the basis of a simple model of the current sheet are the density maxima associated with the sheet "crossing" at $\sim 12 R_J$. This bifurcation of the plasma sheet has previously been noted [24]. Fig. (2) suggests that all three crossings shown exhibit this bifurcated structure. Fig. (1) shows this is clearly the case for the "crossing" at $\sim 21 R_J$. Crossings at $\sim 32 R_J$, $\sim 28 R_J$, and $\sim 25 R_J$ do not indicate similar structure although the decreased signal to noise ratio obscures the variations. Low resolution mode data do suggest the bifurcation at the $28 R_J$ crossing as well as at another crossing at $\sim 36 R_J$. Close inspection of the figures indicates a distinct asymmetry, viz. the second density enhancement in each pair shows more heavy ions as well as protons, the latter being routinely

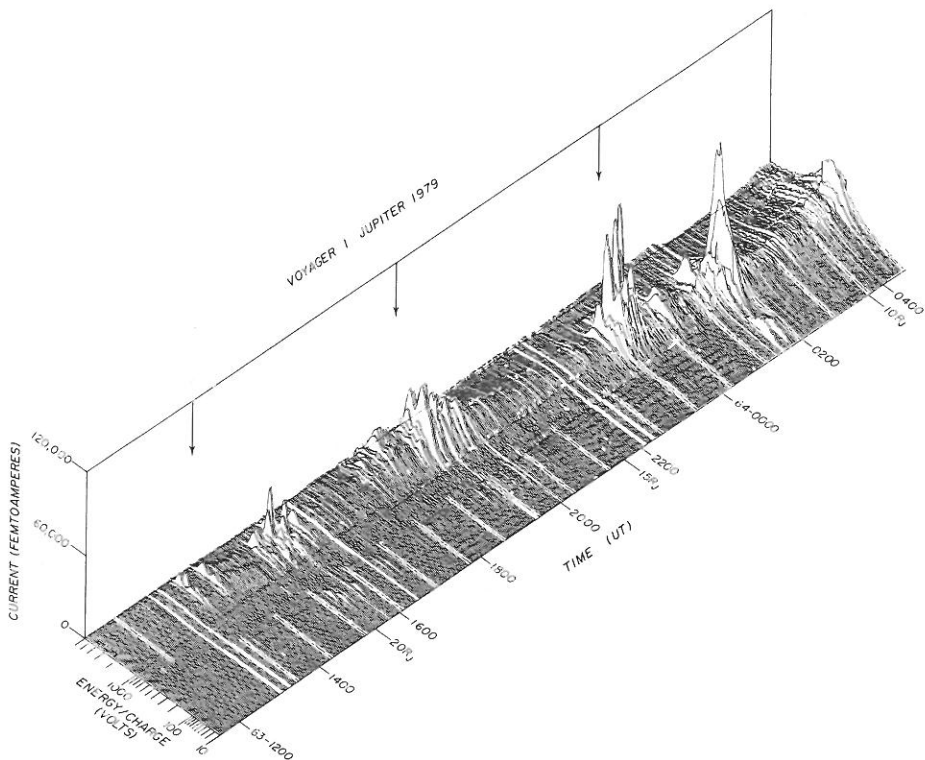


Fig. 2 Same as Fig. (1) but closer to Jupiter. Maximum current displayed is 1.2×10^{-10} amperes ($\sim 1.3 \times 10^7$ electron charges $\text{cm}^{-2} \text{ s}^{-1}$).

discernible only at greatly reduced levels in the low resolution mode data (not shown). The density maxima are not well correlated with crossings of the "centrifugal equator."

It has been reported that flux anisotropies associated with these density maxima of low energy plasma strongly suggest flow along field lines away from the symmetry surface [24,47]. This still seems a viable hypothesis although velocity vector determinations in this "plasma sheet" have yet to be obtained. In any case, the absence of plasma between the two density enhancements at $12 R_J$ is a real effect and appears to track the densities detected in a much higher energy range by the LECP instrument [31].

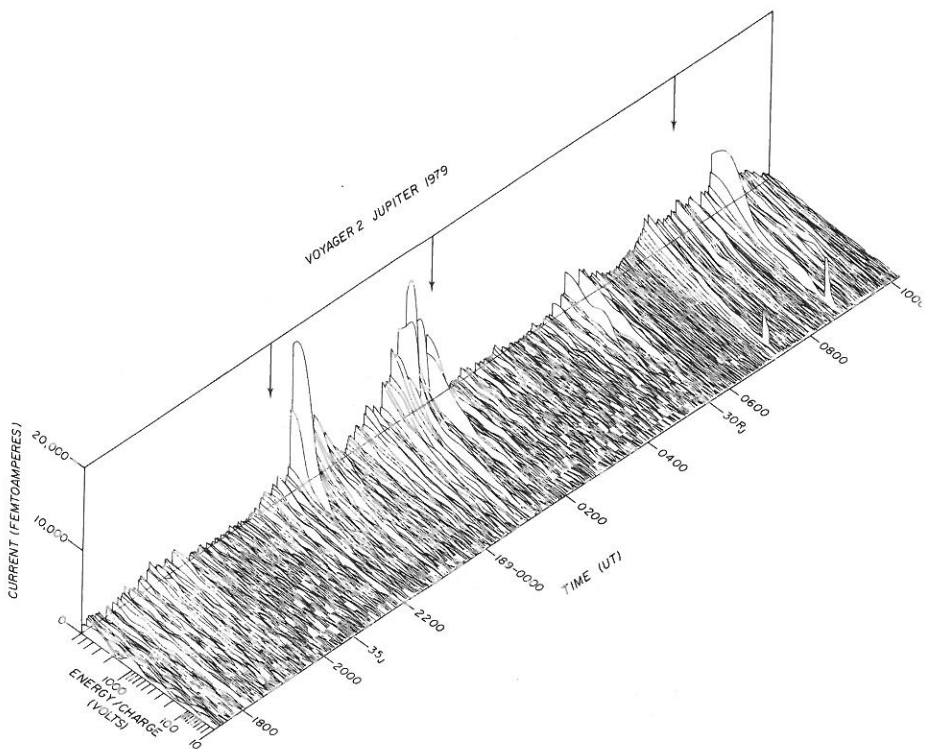


Fig. 3 A cubic spline fit to low resolution mode Voyager 2 data acquired by the side sensor of the PLS experiment. The maximum current displayed is 2×10^{-11} amperes ($\sim 2.2 \times 10^6$ electron charges $\text{cm}^{-2} \text{s}^{-1}$).

The double peak structure is not as visible in the Voyager 2 data at Jupiter. Fig. (3) shows low resolution mode data from Voyager 2 inbound between $\sim 37 R_J$ and $\sim 27 R_J$. Single density enhancements associated with crossings of the magnetic equator are readily apparent. Actual analysis of many of the spectra shown is severely complicated by the fact that only the low energy tail of the heavy ion distributions fell within the energy/charge range of the PLS instrument. Furthermore, proton signatures are not sufficiently above the instrumental noise level to provide good velocity component determinations. It is clear that the first two enhancements depicted lie near the nominal crossings of the magnetic equatorial plane; in addition, the enhancements correlate well with depressions in the magnetic field strength [30]. The enhancement at $30 R_J$ does not correspond to a nominal crossing of the magnetic

equatorial plane, although there is a correlation with the measured field strength. The final crossing in Fig. (3) is much broader in extent and does not show a density maximum at the center of the overall enhancement; however, the plasma sheet is not clearly bifurcated as in the Voyager 1 data discussed above. Closer in, much of the inbound data cold enough to analyze is clearly associated with the Ganymede wake phenomena [48]. There is no other evidence for a bifurcation of the plasma sheet in the Voyager 2 data.

This complex vertical structure of the plasma sheet prevents us from naively applying equations Eqs. (8) and (9) (or their generalizations for multiple ionic species, cf. [49]) in this region of the Jovian magnetosphere. Quantitative analysis of the sheet crossings here must await vector velocity determinations using the full PLS instrument response [50].

Although simple momentum balance apparently does not hold across the symmetry surface in the Jovian magnetosphere, we can still consider simple momentum balance in the symmetry surface. Field-aligned flow at the equator can have important dynamical consequences in this surface. If the component of plasma velocity along the field lines is large enough, there will be an additional outward force density of order $\rho v_s^2/R_c$, where v_s is the component of streaming velocity along the field lines. In this case M_A should be replaced by $M_{A,eff}$ where

$$M_{A,eff} = M_A \left(1 + \frac{\tilde{\omega}}{R_c} \frac{v_s^2}{\tilde{\omega}^2 \Omega^2} \right) \quad (17)$$

At present, we have no reason to believe this correction is appreciable, so we use Eq. (11) without modification in what follows.

A plot of Alfvén Mach number versus radial distance derived from Voyager 1 inbound data shows a pronounced variation as the spacecraft moved between large northerly and large southerly magnetic latitudes [39]. The side sensor of the PLS instrument looked almost in the azimuthal direction, so the full velocity vector not being available [24], the velocity component into the sensor was used to compute M_A . The peak value of M_A derived from Voyager 1 data is between 1 and 2 [39].

During the inbound passage of Voyager 2, the Alfvén Mach number typically had a value between 0.3 and 0.9 in the cold, dense regions, about one-half of the value found during the Voyager 1 encounter at corresponding radial distances.

Only spectra exhibiting very supersonic plasma components have been analyzed. The plasma β scales as the square of the ratio of the Alfvén Mach number to the sonic Mach number, and so we expect the β of the cold ions to be negligible in the dynamical sense. A population of "warm" ions [51] as well as electrons can possibly contribute a plasma β as large as 0.5 [52]. However, most of the plasma pressure in the Jovian magnetosphere outside of the Io torus is due to hot ions, so we ignore the pressure of electrons and ions observed by the PLS instrument in our stress balance calculations.

Barbosa et al. [53] have analyzed LECP data from Voyager 1 outbound (20 R_J to 80 R_J) and found that the pressure varies as

$$P = \alpha \left(\frac{R_J}{\tilde{\omega}} \right)^{3.54} \quad (18)$$

where $\tilde{\omega}$ is the radial distance from Jupiter. Pressure profiles published by Krimigis et al. [31] give a similar exponent for the pressure variation observed by both Voyager 1 and Voyager 2 inbound. The value of α is difficult to determine. Measurements by the LECP instrument which routinely allow calculation of plasma parameters do not allow separation of different ionic species. Barbosa et al. argue that the plasma sheet consists primarily of hot protons and find $\alpha = 6.7 \times 10^{-4}$ ergs cm^{-5} . Lanzerotti et al. [54] have analyzed LECP data obtained from Voyager 2 outbound and conclude that about 75% of the pressure is due to hot protons, the other 25% being due to hot O^+ ions. Assuming all of the LECP signal is in response to O^+ rather than protons increases the estimated pressure by a factor ~ 8 . If we assume the composition deduced by Lanzerotti et al. holds globally, the total pressure is approximately given by Eq. (18) with $\alpha \sim 1.8 \times 10^{-5}$ ergs cm^{-5} . One can obtain values for β at the sheet crossings (field minima), assuming the Voyager 2 outbound composition and using the data of Fig. (24) in [31]. These values (see [39]) have been plotted as discrete points in Fig. (4). For comparison, the value of P can be deduced from the CAN field model by assuming no pressure anisotropy and directly integrating the z-component of Eq. (5), subject to the boundary conditions $P=0$ at $z=D$ [34,41] (however, the presence of a pressure anisotropy at these energies is suggested by Pioneer 10 measurements [55]). We find that the CAN field model predicts a value of β at the symmetry surface given by

$$\beta = \frac{4\pi I_o}{c} \frac{D^2}{B R_c} \quad (19)$$

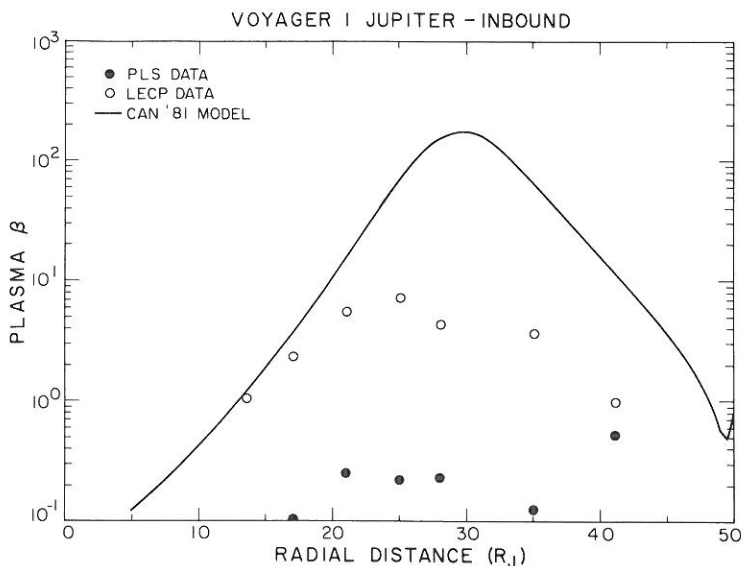


Fig. 4 Comparison of plasma β values from experiment and theory. Discrete points are calculated from PLS and LECP positive ion data using the measured magnetic field values. The solid line is obtained from the CAN '81 model using Eqs. (15) and (16).

This value of β is plotted as the solid curve in Fig. (4). The maximum value of $\beta \sim 175$ occurs for $\omega \sim 29 R_J$. The β values derived from the in situ measurements are consistently low compared to the theoretical values.

In Fig. (5) we have plotted $4\pi\tilde{\omega}J/cB = 4\pi I_o/cB$, which gives the (normalized) inward $\vec{J} \times \vec{B}$ force in the equatorial plane using the CAN model. Discrete points indicate the quantity $M_A^2 + 1.8\beta$ derived from PLS and LECP data obtained by Voyager A_1 inbound. For an isotropic pressure variation given by Eq. (18), (and equilibrium) the outward stress given by this (dimensionless) quantity should just be balanced by the inward Lorentz force (cf. Eq. (11)). However, the Lorentz force produced by the CAN model overwhelms the outward centrifugal and pressure gradient forces outside of $\sim 20 R_J$. This is puzzling, given the good fit between the magnetometer data and the CAN model [40,46]. One could attempt to duplicate the good fit to the magnetometer data and simultaneously lower the Lorentz force by letting the sheet thickness vary with radial distance while varying the sheet parameters [34]. A detailed study of such tradeoffs is beyond the scope of this paper.

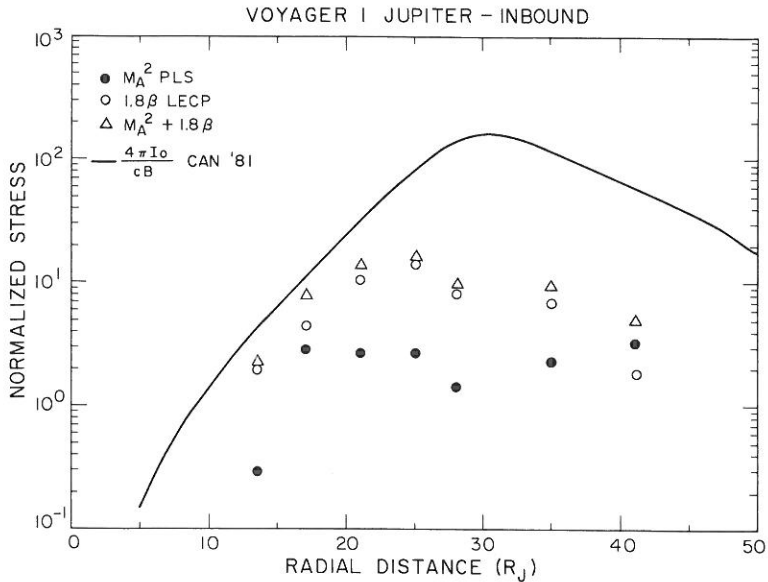


Fig. 5 Comparison of the force exerted on the magnetic field by the pressure gradient of the hot ions and the centripetal acceleration of the cold ions with the Lorentz force predicted by the CAN '81 model magnetic field.

VOYAGER AT SATURN

The near perfect alignment of the magnetic and rotational axes of Saturn should produce a simple scale height distribution of the magnetospheric plasma. Diffusive radial transport should then produce a gradual radial variation of the plasma density near the symmetry plane. However, data returned by the PLS experiments on Voyager 1 and 2 show a smooth variation of density and temperature with distance only inside of about $10 R_S$ (Fig. (6)). Most of the data in this inner region has yet to be analyzed; however, the data which has been analyzed can be compared with a scale height model.

On their inbound trajectories, both Voyager spacecraft traveled further in ω than in z so most of the change in signal observed in Fig. (6) is due to radial variations. However, near periapsis, latitudinal variations are expected to dominate in both Voyager data sets. In a plasma with both light and heavy ions at about the same temperature, the heavy ions should be more concentrated toward the symmetry surface [56].

In the Voyager 1 data shown in Fig. (6), signals from both

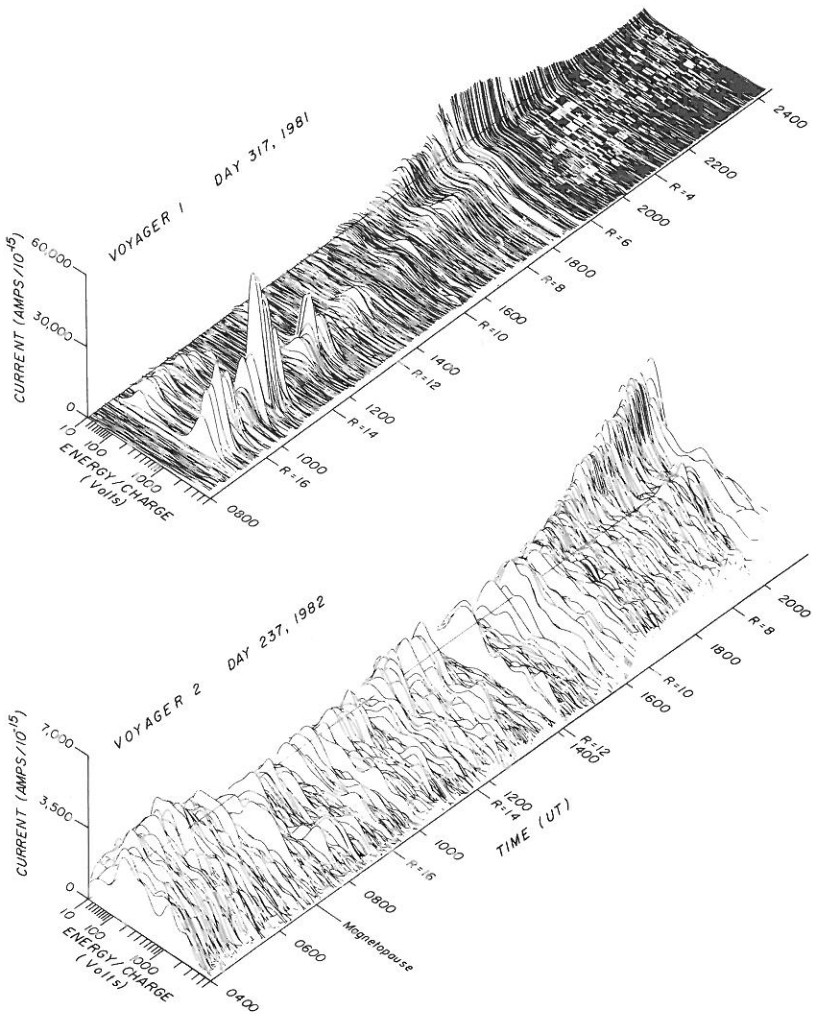


Fig. 6 A cubic spline fit to low resolution mode data acquired by the side sensor of the PLS experiment on the Voyager 1 and Voyager 2 spacecraft during their Saturn flybys. Note the different scales for the measured currents. (6×10^{-11} amperes corresponds to a charge flux density of $\sim 6.7 \times 10^6$ electron charges $\text{cm}^{-2} \text{s}^{-1}$).

protons and heavy ions increase and then decrease inside of 10 R_S . The decrease in proton signal occurs as the corotating protons drop below the energy threshold of the instrument. The

drop in the heavy ion signature could be a latitudinal effect superimposed upon an increase in density with decreasing distance from the planet. In this part of the magnetosphere we expect Dione (at $6.25 R_S$) and Tethys (at $4.88 R_S$) to be the dominant sources of plasma [57], so one would naively expect the density to continue to increase as the spacecraft moved inward. Assuming a dipole field the scale heights for protons and singly charged oxygen ions are $\sim 3 R_S$ and $\sim 2 R_S$, respectively, in this region, but the spacecraft was still within $2 R_S$ of the equator at hour 1900 when the heavy ion signature disappeared. Therefore, the location of the relative density maxima have no simple explanation. This variation was also seen on Voyager 1 outbound as the spacecraft neared the equatorial plane [26]. In both cases, the relative variation of heavy ion signal with respect to that of the protons is apparently a combination of changing sensor response and both radial and vertical density gradients in the plasma distribution. The appreciable radial density gradients preclude a scale height comparison without more analysis beyond the scope of this paper.

Voyager 2 data acquired outbound at the ring plane crossing (not shown) do fit a scale height model. However, a temperature anisotropy $T_{\perp}/T_{\parallel} \sim 5$ is required to fit the data (rigid co-rotation is assumed) [26]. At this distance from Saturn ($2.8 R_S$), the planetary magnetic field clearly dominates the dynamics. (At the density peak of $\sim 130 \text{ cm}^{-3}$ of O^+ , $M_A \sim 6 \times 10^{-2}$ and $\beta_{\perp} \sim 5 \times 10^{-4}$). These observations provide a verification of Eqs. (8) and (9) in this region of the Kronian magnetosphere although the first term on the right hand side of Eq. (9) dominates and the electrons must be taken explicitly into account ($T_e \sim T_{\parallel}$) [26].

Most of the analyzed PLS data at Saturn are cold spectra taken by Voyager 1 inbound between about $17 R_S$ and $10 R_S$, i.e., in the "ring current" region [41]. The spacecraft is close enough to the symmetry surface that outside of $10 R_S$ the value of M_A at Saturn derived from in situ measurements should be close to its value in the equatorial plane [26,39].

We can ignore the pressure of the cold ions at Saturn as we did at Jupiter, and assume that all of the pressure gradient force is due to the hot ion population. Warm ions detected by the PLS instrument, hot ions detected by the LCEP instrument, and electrons detected by the PLS instrument each contribute a value between about 0.1 and unity to the overall plasma β in the vicinity of the ring current [26,58,59,60]. This is in fair agreement with the CAN model for Saturn [41] for which Eq. (19) gives values of β between 0.8 and about 3 (Fig. (7)). Values of the hot ion energy density are shown in Fig. (16) of

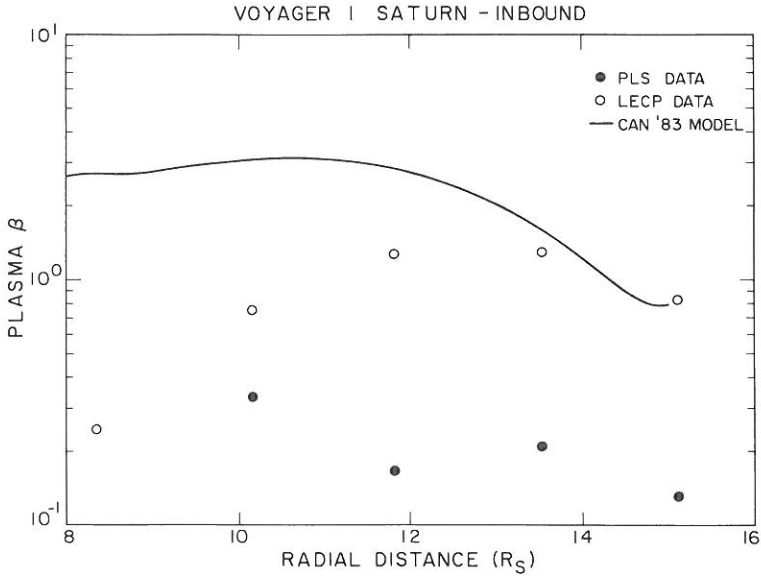


Fig. 7 Comparison of plasma β values from experiment and theory. Discrete points are calculated from PLS and LECP positive ion data using the measured magnetic field values. The solid line is obtained from the CAN '83 model.

[59] for distances between closest approach and $25 R_S$. For Voyager 1 inbound the ratio of ion energy density to magnetic field energy density peaks at $\sim 12.5 R_S$, a distance greater than that of the CAN model peak in β of ~ 3.1 at $10.6 R_S$. Close examination of the LECP data shows that the peak value is $\beta_{LECP} \sim 0.2$ or 1.7 if the composition is assumed to be totally H^+ or O^+ , respectively (N.B. Our definition of β as a pressure ratio is $2/3$ the corresponding energy density ratio which is plotted in [59]).

The overall pressure profile at Saturn is not fit very well by a power law such as Eq. (18). However, for purposes of comparison with the situation at Jupiter we can use the data in Fig. (16) of [59] and estimate

$$P \propto \omega^{-1.6} \quad (20)$$

for Voyager 1 inbound at Saturn in the ring current region. Electron data from the PLS experiment (Fig. 12 of [60]) yields a similar exponent with $\beta_{electron} \sim 0.1$.

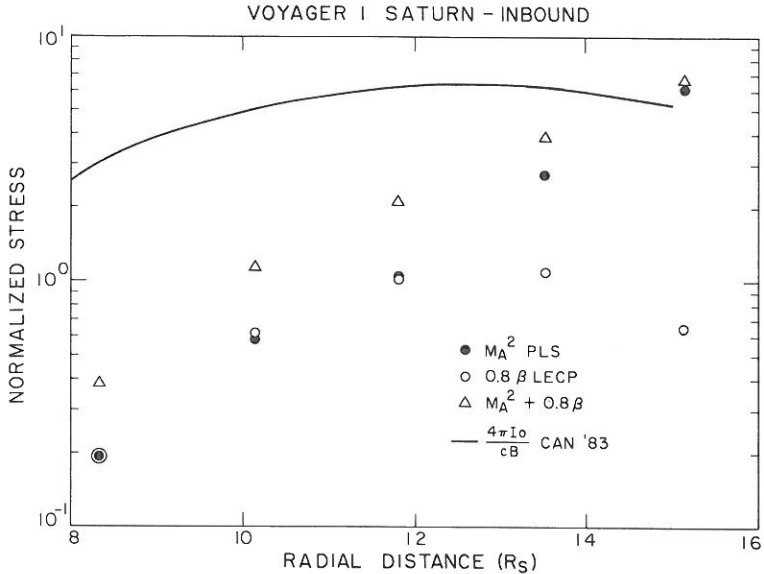


Fig. 8 Comparison of the force exerted on the magnetic field by the pressure gradient of the hot ions and the centripetal acceleration of the cold ions with the Lorentz force predicted by the CAN '83 model magnetic field. The forces have not been corrected for latitudinal variations.

Assuming M_2 isotropy, Eq. (11) predicts a stress from the plasma of $M_A^2 + 0.8\beta$. (Fits of β cold spectra from Voyager 1 inbound in the region $6.3 R_S < \omega < 16.8 R_S$ indicate a mild anisotropy $T_\perp/T_\parallel \sim 1.5$). Alfvén Mach numbers between 2 and 3 and plasma β 's of ≤ 2 clearly indicate that most of the stress on the field lines at Saturn results from the corotating cold plasma. This is precisely the situation originally postulated as occurring at Jupiter [10]. Inflation of the magnetosphere by hot plasma, the dominant effect at Jupiter, is of only secondary importance at Saturn.

To quantify the cross field stress balance in the Kronian magnetosphere, we have made a plot similar to that shown in Fig. (5). In Fig. (8) discrete points show the quantities M_A^2 , 0.8β and their sum using data from Fig. (16) of [59] and from Fig. (17) of [26]. Although the data were taken at larger and larger distances from the symmetry surface as the spacecraft approached the planet, we have made no attempt to correct for any latitudinal dependance in M_A or β .

The agreement between the inferred stress and that predicted with the CAN model field is much better at Saturn than at Jupiter. The unmodeled latitudinal dependence is pronounced; the centrifugal force becomes less important and the pressure gradient force more important as the spacecraft nears the planet and reaches higher latitudes. There is apparently an excess of inward Lorentz force in the model. At least some of the discrepancy can be ascribed to our use of values of M_A^2 obtained "away from" the equatorial plane. In addition, the actual current carrying region appears to extend to larger distances and to be stronger at these distances than the CAN '83 model implies, suggesting that a different ring current extent and/or thickness might provide better agreement with the data.

Part of the difference may be due to the model field being based upon the flybys of both Voyager spacecraft on both their inbound and outbound legs; the plasma data is from Voyager 1 inbound only. (Voyager 2 did not fly through the current carrying region as did Voyager 1 [41]). In the region between $\sim 8 R_S$ and $18 R_S$ the Voyager 1 spacecraft moved $\sim 0.3 R_S$ to $1.7 R_S$ away from the equatorial plane. This is roughly three quarters of a scale height for the heavy ions and less for the protons [26]. This suggests that the latitudinal variation in plasma properties should be small and that there is a real discrepancy between the Lorentz force produced by the model and that inferred from the data. A more quantitative assessment requires modeling the latitudinal dependence of M_A , and/or a more detailed study of the tradeoffs in the parameters of the CAN model.

VOYAGER AT URANUS

The Voyager 2 spacecraft will fly through the Uranian system in January, 1986 passing within $\sim 4.5 R_U$ ($1 R_U = 25,400$ km) of the planet [61]. A surface magnetic field comparable to that of Jupiter or Saturn has been inferred [23] from observations of excess Lyman- α radiation coming from Uranus [19,20]. (Presumably the UV excess is auroral, implying the existence of a magnetic field). This inferred field strength would suffice to stand off the solar wind to at least $30 R_U$, placing the five known moons within a Uranian magnetosphere. Simply using Blackett's relation [62] and normalizing to Saturn's magnetic moment produces a standoff distance of only $\sim 11 R_U$ at times of high solar wind dynamic pressure and $\sim 25 R_U$ at times of low pressure. Such a magnetosphere would still always contain the large moons, Ariel and Umbriel.

A Uranian magnetosphere may be relatively empty. It has been argued that the planetary ionospheres and solar wind should provide even less plasma to the magnetospheres of Uranus

and Neptune than they do to those of Jupiter and Saturn [63]. The interstellar wind (of neutral atoms) may provide a significant amount of magnetospheric plasma at Uranus and Neptune; however, this source should be active at Jupiter and Saturn as well, but its presence at these planets has yet to be confirmed [21]. On the other hand, a "self-generating" sputtering mechanism could provide a significant internal plasma source. The four large moons of Uranus are of comparable size to the medium sized icy moons of Saturn (Fig. (9)). The latter, especially Dione and Tethys, apparently supply a significant part of the ring current plasma to Saturn's magnetosphere via the sputtering of water ice from their surfaces [56,57,64,65]. Detection of water frost on the Uranian moons [66,67,68] suggests that sputtering could provide a source of oxygen ions and protons to the Uranian magnetosphere [69,70]. Dark material on the surfaces of the moons may contain elemental carbon [65] or more complex organic compounds produced by the sputtering of methane ice [69]. This material could be a source for injection of carbon ions as well into the magnetosphere.

COMPARISON OF SYSTEMS

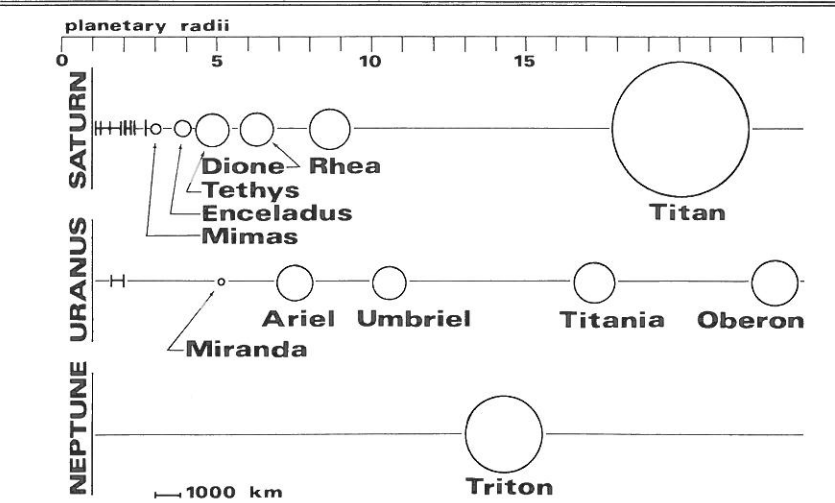


Fig. 9 Comparison of the planetary systems of Saturn, Uranus, and Neptune. Distances of the centers of the moons from their respective planets are scaled in units of planetary radii. Diameters of all of the moons are scaled to a common length. Locations of the inner and outer edges of the main rings of Saturn and of the ring system of Uranus are indicated by vertical bars.

The "pole-on" orientation of Uranus at the time of the Voyager 2 encounter will limit in situ measurements to a fairly constant distance from the planetary spin axis, while a large range of distances from the equatorial plane will be sampled. Particle measurements yielding high values of β and/or high values of M_A for heavy ions, indicative of a ring current or current sheet, will be possible but severely limited in spatial coverage [71]. The onboard magnetometer will sample only briefly, if at all, the signature of a ring current system. If the plasma sources and current system are as strong as they are at Saturn (at comparable distances in the equatorial plane), they should be detectable by the Voyager experiments. However, little of the overall plasma structure perpendicular to the field will be directly sampled.

VOYAGER AT NEPTUNE

The final planetary encounter of Voyager 2 will occur in September, 1989 as the spacecraft passes $\sim 0.4 R_N$ ($1 R_N = 24,300$ km) over the north pole of Neptune [61]. Neptune is similar in size to Uranus and may have a similar rotation period [72], but neither radio nor optical evidence for a Neptunian magnetic field has been found. Like Jupiter and Saturn (but unlike Uranus), Neptune does exhibit an infrared excess [72] which has been associated with the presence of intrinsic planetary magnetic fields. Blackett's relation (normalizing to Saturn's magnetic moment) predicts an equatorial magnetic field strength ~ 0.05 G, about that obtained for Uranus by this method. Predicted solar wind standoff distances are somewhat greater owing to Neptune's greater distance from the sun: $13 R_N$ to $30 R_N$ at times of high and low solar wind dynamic pressure, respectively. (Pioneer 10, now outside of Neptune's orbit, is still detecting large variations in solar wind ram pressure comparable to those observed by Voyager 2 at ~ 13 AU [73]).

The Neptunian system is quite different from those of the other outer planets. The one large satellite Triton is in an inclined, retrograde orbit at $\sim 14 R_N$. Intermediate in size between the medium icy satellites and the Galilean satellites, Triton was thought to have a tenuous methane atmosphere consistent with the vapor pressure of methane ice at 55 K. There is no compelling evidence for methane frost on the surface [74], and recent studies of infrared spectra of Triton suggest the moon may be covered by an "ocean" of liquid nitrogen and an atmosphere with a surface pressure of ~ 0.1 bar [75].

McDonough and Brice found that a Triton gas torus, similar to that of Titan, is a possibility [76]. Voyager 1 measure-

ments have shown that Titan is an important source of both nitrogen and protons for Saturn's magnetosphere, despite the fact that the location of the moon in or out of the magnetosphere is a function of solar wind ram pressure. Similarly, Triton may supply a neutral gas torus of atomic hydrogen and/or neutral atoms to the Neptunian system. However, the lifetime of such a neutral torus against ionization via solar wind charge exchange and photoionization at Neptune is about ten times that at Saturn [76], so a torus similar to that of Titan could be produced with only a tenth of the source strength at Titan. Depending upon the actual magnetic moment of Neptune, Triton and an associated torus could spend part of the time in the magnetosphere, part in the magnetosheath, and part in the solar wind as do Titan and its torus. A Tritonian torus could, therefore, supply heavy ions and protons internally to a Neptunian magnetosphere, although perhaps with a source strength smaller than that at Saturn. Because Triton's orbital plane is tilted some 20° to the equatorial plane of Neptune, plasma injection (upon ionization and pickup) would occur in a much larger volume of space than at the other outer planets.

The planned Voyager 2 encounter trajectory at Neptune is similar to the Voyager 1 outbound leg at Saturn. The spacecraft will pass through the equatorial plane twice at $\sim 3.6 R_N$ inbound and $\sim 5.3 R_N$ outbound [61]. Spatial coverage of the equatorial region will be much better than at Uranus. If a significant amount of plasma diffuses inward from Triton, it should be detectable at the magnetic symmetry surface. If the radial gradients are not great, it may be possible to deduce the scale height of the plasma sheet. In situ measurements of the magnetic field as well as inferred values of β and M_A can be used as "tracers" for a ring current. On the outbound leg of its encounter Voyager 2 will fly parallel to Triton's orbital plane $\sim 1 R_N$ from it [61]. If Triton injects plasma continuously into a Neptunian magnetosphere, it may be possible to detect the resultant plasma distribution during part of Voyager's outbound traverse of the magnetosphere.

The outermost known planet in the solar system, Pluto, is similar in size and spectral signature to Triton [77]. Pluto apparently has a tenuous methane atmosphere [78] and, like the other medium-sized moons in the solar system, probably has no intrinsic magnetization. As there are no plans for a spacecraft flyby of Pluto in this century, Voyager observations of Triton and its interaction with the solar wind and/or a Neptunian magnetosphere, will, for the foreseeable future, provide our best guesses for the interaction of Pluto with its plasma environment.

DISCUSSION

Spacecraft encounters with two of the four giant planets in the solar system have revealed corotation-dominated magnetospheres (rather than convection dominated as at Earth). In addition, the moons of Jupiter and Saturn provide a sufficiently strong internal source of plasma that strong current systems are formed, which significantly perturb the vacuum magnetic field of those planets. We have shown the plausibility of similar magnetospheres at Uranus and Neptune, a hypothesis which will be tested by the Voyager 2 spacecraft before 1990.

Ideally, one would like to use the magnetospheres of the giant planets in a comparative sense to investigate the general problem of the MHD equilibrium of plasma confined by a fast magnetic rotator. One scaling law which holds for the earth, Jupiter, and Saturn relates the ring current perturbation field ΔB to the planetary equatorial field strength B_e by [41]:

$$\Delta B \sim 5 \times 10^{-4} B_e \quad (21)$$

If this scaling holds at Neptune and Uranus, a limiting value for the total energy which can be stably contained by the planetary field is implied. That conclusion follows from the non-linear generalization of the Dessler-Parker relation (which can be derived from Eq. (1)) [79]:

$$\frac{E}{U} + \frac{1}{2} \frac{U_{\text{self}}}{U} = \frac{3}{2} \frac{\Delta B}{B_e} \quad (22)$$

Here E is the total particle energy, U is the energy in the dipole part of the magnetic field and U_{self} is the energy in the non-dipolar part. However, this relationship does not suffice to determine E as a function of U_{self} .

The division of energy can be determined given a model field and particle distribution which obeys Eqs. (1)-(4). A restricted model is that of Parker and Stewart which is valid for hot isotropic plasma in a non-rotating magnetosphere [80]. A similarity solution for this model exhibits a maximum in the stably confined particles for $B_z(z=0) \sim r^{-2.4}$. The ratio of particle energy to magnetic field energy in the vacuum dipole is about 0.2 while the total energy in the field is approximately that of the dipole case. For this model, the non-linear Dessler-Parker relation then gives

$$\Delta B_{\text{MAX}} \sim 1.3 \times 10^{-1} B_e \quad (23)$$

This strongly suggests that the maximum current, and hence ΔB , which can be contained by the Jovian and Kronian magnetospheres is determined by factors other than simple MHD equilibria criteria, e.g., stability with respect to flux tube interchange [81] (and references therein).

It is interesting to note that the Parker and Stewart similarity model predicts a value of β in the equatorial plane which is only a function of the similarity parameter and its corresponding eigenvalue. For the case of maximum inflation (corresponding to ΔB_{MAX} in Eq. (23)), $\beta \approx 2.9$, approximately the value predicted by the CAN '83 model for Saturn (see Fig. (7)), even though Eq. (23) does not hold.

There have been numerous attempts to model rapidly rotating magnetospheres, primarily with Jupiter in mind [34] (and references therein), [82]-[86]. Some approximations must be made to make the problem tractable, and these usually involve an expansion of Eqs. (1)-(4) in the ratio of the centrifugal to the pressure gradient force. An alternate approach is to attempt to find the pressure and density separately. The latter has been done using the CAN '81 model field at Jupiter [34] and by using a similarity technique with a finite corotation lag [83]. These treatments yield average plasma temperatures of ~ 5 keV and ~ 10 keV, respectively. This is consistent with the temperature range inferred at Jupiter by Barbosa et al. [53] and predicted at Jupiter by Goldstein [12] and Goertz [13] on the basis of a model magnetic field derived from Pioneer 10 data. The observed near constancy of the average temperature with radial distance is consistent with the observed corotation lag at Jupiter [83].

As emphasized by Cheng [83], the temperature is an average over at least two particle populations, one hot and one cold [87]. This applies at both Jupiter and Saturn. In some average sense, the agreement between the model temperatures and those inferred from in situ measurements must be indicative of the "goodness of fit" of the model magnetic field to the actual field generated by the planet and its current sheet. In terms of β and M_A the temperature is given by

$$kT = \frac{1}{2} m v^2 \beta / M_A^2 \quad (24)$$

where v is the bulk speed of the plasma.

Using the values shown in Fig. (4) and Fig.(5) for β and M_A at Jupiter, $m \sim 15$ amu and $v \sim 200$ km/s (see e.g. [24]), we obtain $kT \sim 9$ keV for $20 R_J \leq \tilde{\omega} \leq 40 R_J$. The factor of 2 difference in the effective temperature derived from the data and

the CAN '81 magnetic field model is related to the excessive Lorentz force provided by the model current sheet. The data from Saturn shown in Figs. (7) and (8) give an effective temperature of ~ 1 keV ($m \sim 15$ amu and $v \sim 150$ km/s in the ring current region [26]). Using the data of Figs. (9) and (10) in [41], we find that the CAN '83 model predicts a plasma temperature of ~ 1.5 keV at the inner edge of the ring current and ~ 0.5 keV at the outer edge. Again, the agreement between the model and the data is much better at Saturn than at Jupiter.

This emphasizes that for the magnetospheres of Jupiter and Saturn, the heating of the magnetospheric plasma is different in the two cases. Whether this is due only to the much greater mass injection at Jupiter as compared to that at Saturn remains unclear. Despite the apparent MHD equilibrium of both magnetospheres, the ring current structures differ in both magnitude and shape. This implies the difference between these current systems is due to not only the difference in mass injection but also to differences in the effective equation of state (i.e., the effective temperature), which, in turn, may be influenced by the location of the plasma source(s).

In situ measurements at Uranus and Neptune should help quantify the "equation of state" problem and its relationship to MHD equilibrium, if sufficient plasma and magnetic field data is acquired. The Uranian moons bear a resemblance to the icy moons of Saturn; Triton may provide a gas torus at Neptune similar to that of Titan at Saturn. Therefore, the magnetospheres of these two planets may mimic the inner and outer parts of Kronian magnetosphere. Intercomparison of these three outer planet magnetospheres could provide a better understanding of plasma injection and heating at Saturn and how these processes and the requirements of force balance interact with each other.

SUMMARY

We have investigated the conditions of force (or stress) balance in corotation-dominated planetary magnetospheres by comparing appropriate parameters derived from in situ spacecraft measurements. We first derived a simplified version of the MHD momentum equation appropriate near the symmetry surface of such planetary magnetospheres, including terms produced by arbitrary field line curvature and pressure anisotropy. We used particle and plasma data acquired by the Voyager spacecraft at Jupiter and Saturn to compute approximate values of the plasma β , the Alfvén Mach number, and the pressure gradient. Using these quantities and the current sheet models used for fitting the Voyager magnetometer data during the

planetary encounters, we found that these models overestimate the Lorentz force at Jupiter and Saturn and underestimate the temperature in the plasma sheet at Jupiter.

A qualitative state of corotating MHD equilibrium is strongly suggested. Reasons for the quantitative discrepancies are unclear given the good fit between the model magnetic field and magnetometer data. The equilibria which are obtained are affected by the current sheet configurations and plasma temperature. These properties are not determined by equilibrium conditions alone, but by other physical processes.

Data from the upcoming Voyager encounters with Uranus and Neptune may help clarify the general problem of the MHD equilibrium of rotating magnetospheres as well as specific problems such as that of the location of the sources of plasma at Saturn.

ACKNOWLEDGMENTS

The author wishes to acknowledge helpful discussions with and comments on the manuscript by H. S. Bridge and J. W. Belcher. The author wishes to thank the Voyager magnetometer team (N. Ness, Principal Investigator) for making available magnetic field data acquired at Jupiter and Saturn, A. Bowes for preparing the manuscript and T. Chang for his patience and encouragement.

This work was supported under NASA contract 953733 to the Jet Propulsion Laboratory.

REFERENCES

- [1] V. C. A. Ferraro, *Mon. Not. Roy. Astron. Soc.* 97, 458 (1937).
- [2] L. Davis, Jr., *Phys. Rev.* 72, 632 (1947).
- [3] L. Davis, Jr., *Phys. Rev.* 73, 536 (1948).
- [4] J. W. Dungey, "Cosmic Electrodynamics," (Cambridge University Press, Cambridge, 1958, p. 64).
- [5] T. Gold, "Space Exploration and the Solar System," ed. B. Rossi, (Academic Press, New York, 1964, p. 192).
- [6] C. F. Kennel and F. V. Coroniti, *Space Sci. Rev.* 17, 857 (1975).
- [7] T. W. Hill, *J. Geophys. Res.* 84, 6554 (1979).
- [8] J. H. Piddington, "Cosmic Electrodynamics," (John Wiley and Sons, Inc., New York, 1969, p. 197).
- [9] N. M. Brice and G. A. Ioannidis, *Icarus* 13, 173 (1970).
- [10] E. J. Smith, L. Davis, Jr., D. E. Jones, P. J. Coleman, Jr., D. S. Colburn, P. Dyal, C. P. Sonett, and A. M. A. Frandsen, *J. Geophys. Res.* 79, 3501 (1974).
- [11] C. K. Goertz, D. E. Jones, B. A. Randall, E. J. Smith, and M. F. Thomsen, *J. Geophys. Res.* 81, 3393 (1976).
- [12] H. Goldstein, *Planet. Space Sci.* 25, 673 (1977).
- [13] C. K. Goertz, *Space Sci. Rev.* 23, 319 (1979).
- [14] R. J. Walker, M. G. Kivelson, A. W. Schardt, *Geophys. Res. Lett.* 5, 799 (1978).
- [15] F. L. Scarf, *Cosmic Elect.* 3, 437 (1973).
- [16] G. L. Siscoe, *The Saturn System*, ed. D.M. Hunten and D. Morrison (NASA Conference Publication 2068, 1978, p. 265).
- [17] L. A. Frank, B. G. Burek, K. L. Ackerson, J. H. Wolfe, and J. D. Mihalov, *J. Geophys. Res.* 85, 5695 (1980).

- [18] E. J. Smith, L. Davis, Jr., D. E. Jones, P. J. Coleman, Jr., D. S. Colburn, P. Dyal, and C. P. Sonett, *J. Geophys. Res.* 85, 5655 (1980).
- [19] S. T. Durrance and H. W. Moos, *Nature* 299, 428 (1982).
- [20] J. T. Clarke, *Ap. J. Lett.* 263, L105 (1982).
- [21] G. L. Siscoe, "Solar System Plasma Physics," Vol. II, ed. C. F. Kennel et al. (North-Holland, Amsterdam, 1979, p. 319).
- [22] G. L. Siscoe, *Icarus* 24, 311 (1975).
- [23] T. W. Hill, A. J. Dessler, and M. E. Rassbach, *Planet. Space Sci.* 31, 1187 (1983).
- [24] R. L. McNutt, Jr., J. W. Belcher, and H. S. Bridge, *J. Geophys. Res.* 86, 8319 (1981).
- [25] J. F. Carbary, S. M. Krimigis, E. P. Keath, G. Gloeckler, W. I. Axford, and T. P. Armstrong, *J. Geophys. Res.* 86, 8285 (1981).
- [26] A. J. Lazarus and R. L. McNutt, Jr., *J. Geophys. Res.* 88, 8831 (1983).
- [27] R. L. McNutt, Jr., 5th Conference on the Physics of the Jovian and Saturnian Magnetospheres, (M.I.T., June 21-24, 1983).
- [28] J. F. Carbary, B. H. Mauk, and S. M. Krimigis, *J. Geophys. Res.* 88, 8937 (1983).
- [29] M. H. Acuña, J. E. P. Connerney, and N. F. Ness, *J. Geophys. Res.* 88, 8771 (1983).
- [30] N. F. Ness, M. H. Acuña, R. P. Lepping, L. F. Burlaga, K. W. Behannon, and F. M. Neubauer, *Science* 204, 982 (1979).
- [31] S. M. Krimigis, J. F. Carbary, E. P. Keath, C. O. Bostrom, W. I. Axford, G. Gloeckler, L. J. Lanzerotti, and T. P. Armstrong, *J. Geophys. Res.* 86, 8227 (1981).
- [32] J. W. Dungey, *M.N.R.A.S.* 113, 180 (1953).
- [33] I. Lerche and B. C. Low, *Physica* 4D, 293 (1982).

- [34] V. M. Vasyliunas, "Physics of the Jovian Magnetosphere," ed. A. J. Dessler (Cambridge University Press, New York, 1983, p. 395).
- [35] T. W. Hill, *Science* 207, 301 (1980).
- [36] G. L. Siscoe and D. Summers, *J. Geophys. Res.* 86, 8471 (1981).
- [37] T. W. Hill and F. C. Michel, *J. Geophys. Res.* 81, 4561 (1976).
- [38] G. L. Siscoe, *J. Geophys. Res.* 82, 1641 (1977).
- [39] R. L. McNutt, Jr., *Adv. Space Res.* 3, 55 (1983).
- [40] J. E. P. Connerney, M. H. Acuña, and N. F. Ness, *J. Geophys. Res.* 86, 8370 (1981).
- [41] J. E. P. Connerney, M. H. Acuña, and N. F. Ness, *J. Geophys. Res.* 88, 8779 (1983).
- [42] I. S. Gradshteyn and I. M. Ryzhik, *Table of Integrals, Series, and Products* (Academic Press, New York, p. 904).
- [43] H. S. Bridge, J. W. Belcher, R. J. Butler, A. J. Lazarus, A. M. Mavretic, J. D. Sullivan, G. L. Siscoe, and V. M. Vasyliunas, *Space Sci. Rev.* 21, 259 (1977).
- [44] S. M. Krimigis, T. P. Armstrong, W. I. Axford, C. O. Bostrom, C. Y. Fan, G. Gloeckler, and L. J. Lanzerotti, *Space Sci. Rev.* 21, 329 (1977).
- [45] T. W. Hill, A. J. Dessler, and F. C. Michel, *Geophys. Res. Lett.* 1, 3 (1974).
- [46] J. E. P. Connerney, M. H. Acuña, and N. F. Ness, NASA TM-83882 (1981).
- [47] J. W. Belcher and R. L. McNutt, Jr., *Nature* 287, 813 (1980).
- [48] H. S. Bridge, J. W. Belcher, A. J. Lazarus, J. D. Sullivan, F. Bagenal, R. L. McNutt, Jr., K. W. Ogilvie, J. D. Scudder, E. C. Sittler, V. M. Vasyliunas, and C. K. Goertz, *Science* 206, 972 (1979).
- [49] F. Bagenal and J. D. Sullivan, *J. Geophys. Res.* 86, 8447 (1981).

- [50] A. S. Barnett, Ph.D. Thesis, Department of Physics, M.I.T., Cambridge, MA (1983).
- [51] J. D. Sullivan, EOS 62, 1001 (1981).
- [52] J. D. Scudder, E. C. Sittler, Jr., H. S. Bridge, J. Geophys. Res. 86, 8157 (1981).
- [53] D. D. Barbosa, D. A. Gurnett, W. S. Kurth, and F. L. Scarf, Geophys. Res. Lett. 6, 785 (1979).
- [54] L. J. Lanzerotti, C. G. MacLennan, S. M. Krimigis, T. P. Armstrong, K. Behannon, R. P. Lepping, and N. F. Ness, Geophys. Res. Lett. 7, 817 (1980).
- [55] T. G. Northrop, T. J. Birmingham, and A. W. Schardt, J. Geophys. Res. 84, 47 (1979).
- [56] A. Eviatar, R. L. McNutt, Jr., G. L. Siscoe, and J. D. Sullivan, J. Geophys. Res. 88, 823 (1983).
- [57] A. Eviatar, submitted to J. Geophys. Res. (1983).
- [58] C. G. MacLennan, L. J. Lanzerotti, S. M. Krimigis, and R. P. Lepping, J. Geophys. Res. 88, 8817 (1983).
- [59] S. M. Krimigis, J. F. Carbary, E. P. Armstrong, L. J. Lanzerotti, and G. Gloeckler, J. Geophys. Res. 88, 8871 (1983).
- [60] E. C. Sittler, Jr., K. W. Ogilvie, and J. D. Scudder, J. Geophys. Res. 88, 8847 (1983).
- [61] E. C. Stone, Voyager 2 Observations at Uranus and Neptune, Presentation, July 6, 1982.
- [62] P. M. S. Blackett, Nature 159, 658 (1947).
- [63] G. -H. Voigt, T. W. Hill, and A. J. Dessler, Ap. J. 266, 390 (1983).
- [64] A. F. Cheng, L. J. Lanzerotti, and V. Pirronello, J. Geophys. Res. 87, 4567 (1982).
- [65] L. J. Lanzerotti, C. G. MacLennan, W. L. Brown, R. E. Johnson, L. A. Barton, C. T. Reimann, J. W. Garrett, and J. W. Boring, J. Geophys. Res. 88, 8765 (1983).
- [66] D. P. Cruikshank and R. H. Brown, Icarus 45, 612 (1981).

- [67] B. T. Soifer, G. Neugebauer and K. Matthews, *Icarus* 45, 612 (1981).
- [68] R. H. Brown, *Icarus* 56, 414 (1983).
- [69] A. F. Cheng, Proceedings of the Voyager Uranus/Neptune Workshop, Pasadena, CA, 6-8 February, 1984.
- [70] A. F. Cheng and T. W. Hill, Proceedings of the Voyager Uranus/Neptune Workshop, Pasadena, CA, 6-8 February, 1984.
- [71] J. W. Belcher, R. L. McNutt, Jr., and H. S. Bridge, MIT Space Plasma Group Internal Memorandum #87 (1982).
- [72] L. Trafton, *Rev. Geophys. Sp. Phys.* 19, 43 (1981).
- [73] P. Gazis, private communication.
- [74] D. P. Cruikshank and P. M. Silvagio, *Ap. J.* 233, 1016 (1979).
- [75] D. P. Cruikshank, Proceedings of the Voyager Uranus/Neptune Workshop, Pasadena, CA, 6-8 February 1984.
- [76] T. R. McDonough and N. M. Brice, *Icarus* 20, 136 (1973).
- [77] D. Morrison, D. P. Cruikshank, and R. H. Brown, *Nature* 300, 425 (1982).
- [78] U. Fink, B. A. Smith, D. C. Benner, J. R. Johnson, and H. J. Reitsema, *Icarus* 44, 62 (1980).
- [79] R. L. Carovillano and G. L. Siscoe, *Rev. Geophys. Sp. Phys.* 11, 289 (1973).
- [80] E. N. Parker and H. A. Stewart, *J. Geophys. Res.* 86, 8471 (1981).
- [81] G. L. Siscoe and D. Summers, *J. Geophys. Res.* 86, 8471 (1981).
- [82] Z. X. Liu, *J. Geophys. Res.* 87, 1691 (1982).
- [83] A. F. Cheng, *J. Geophys. Res.* 88, 13 (1983).
- [84] O. Kaburaki, *Astrophys. Sp. Sci.* 92, 113 (1983).
- [85] T. Sato and M. Murakami, *Geophys. Res. Lett.* 10, 1120 (1983).

- [86] P. A. Bespalov and Yu. V. Chugunov, *Planet. Sp. Sci.* 32, 365 (1984).
- [87] J. W. Belcher, C. K. Goertz, and H. S. Bridge, *Geophys. Res. Lett.* 7, 17 (1980).